Mitigation of Voltage and Frequency Oscillations of a Microgrid during Wind Gust by Using Fuzzy-Controlled Flywheel Energy Storage

Mouaz Zobair
Electrical Engineering Department,
Aswan Faculty of Engineering,
Aswan University
Aswan, Egypt
mouaz.zobair@eng.aswu.edu.eg

Mohamed M. Aly
Electrical Engineering Department,
Aswan Faculty of Engineering,
Aswan University
Aswan, Egypt
mohamed.aly@eng.aswu.edu.eg

Sayed M. Said
Electrical Engineering Department,
Aswan Faculty of Engineering,
Aswan University
Aswan, Egypt
sayed.said@aswu.edu.eg

***Abstract*— Optimal operation of distributed energy resources (DERs) becomes one of the most critical aspects in the planning of microgrid systems as a result of energy policies aimed at increasing the integration of renewable energies, lowering fossil fuel use, and reducing the environmental effect. Due to the integration of a significant amount of renewable energy sources (RESs), the system inertia in such microgrids is reduced, which negatively affects frequency and voltage stability and weakens the microgrid. The use of Energy Storage Systems (ESSs) significantly lowers voltage and frequency variations. One of the most popular energy storage devices is the Flywheel Energy Storage System (FESS) which is used in this study to tackle the voltage and frequency variations. Among the benefits of FESS over other ESSs are its low maintenance costs, lengthy service life, lack of pollutants, high energy storage, quick charging, and limitless charge/discharge times. FESS has been controlled using a developed fuzzy logic controller that improves microgrid voltage and frequency. The studied power system model is implemented by the MATLAB/Simulink platform. The impacts of wind speed and load variations are examined in this study where voltage and frequency responses are compared in several scenarios. The proposed method displays a significant improvement in the voltage and frequency of the microgrid system. The obtained outcomes show that the fuzzy-controlled FESS is effective in reducing the voltage and frequency fluctuations of the studied microgrid system and keeping their values within the acceptable international standard limitation.**

Keywords*: *Flywheel energy storage, fuzzy logic control, isolated microgrids, wind energy. Introduction

Abbreviations:

DERs	***Distributed Energy Resources***
DFIG	***Doubly Fed Induction Generator***
DFIM	***Doubly Fed Induction Machine***
DG	***Diesel Generator***
ESSs	***Energy Storage Systems***
FESS	***Flywheel Energy Storage System***
FLC	***Fuzzy Logic Control***
GSC	***Grid Side Converter***
MF	***Membership Function***
PMSG	***Permanent Magnet Synchronous Generator***
RESs	***Renewable Energy Sources***
RSC	***Rotor Side Converter***
SMES	***Superconducting Magnetic Energy Storage***
VSC	***Voltage Source Converter***
WECSs	***Wind Energy Conversion Systems***

I. INTRODUCTION

Over the past few decades, the impacts of global warming, the need to minimize pollution, and the heavy dependence on fossil fuels have helped in the development of alternative energy sources based on renewable technologies [1]. In fact, renewable energies, such as wind, sun, bioenergy, and hydropower, provide the best solution for energy sources due to their long-term sustainability and diversity [2].

Among all renewable energy sources (RESs), wind energy is currently the fastest-growing economical energy source in the world [3], [4]. On the other hand, power generated by wind turbines is highly unpredictable, so it is subjected to fluctuations due to wind speed variations. This fluctuating power can produce voltage and frequency variations and reduce the grid's reliability therefore, its inclusion in power networks can cause issues with system operation and planning [5]. In recent years, renewable energy has been used to supply the need for power, particularly in remote locations that may be cut off from the power grid [6].

In remote areas, power generation, which is based on the microgrid's concept using DERs such as wind power generation is a very useful alternative to deliver electric energy [7] [8]. Recently, several methods have been suggested to enhance the quality of the power produced by wind power systems including the use of (ESSs). When the amount of power generated is greater than the demand, the surplus is stored in the ESSs whereas, if the amount of power generated is lower than the demand, the system uses the stored power to cover the deficit. The ESSs can also be adjusted to provide load voltage control and power regulation [9][10][11]. Batteries, fuel cells, superconducting magnetic energy storage (SMES), FESSs, and supercapacitors are examples of energy storage technologies that can be combined in a wind system for power smoothing [12].

ISSN: 2636 - 3712 (Printed Version)
ISSN: 2636 - 3720 (Online Version)

Compared to other energy storage techniques, FESS offers the benefits of being pollution-free, having a long lifespan, being highly efficient and simple to install and maintain, etc. Recently, it has received extensive study and applied in the field of power systems [10].

Several studies have been conducted on the integration of FESS grid-connected and isolated modes of microgrid operation. Authors in [13] created coordinated control strategies for a DFIG and a FESS. It has been suggested to use a fuzzy logic control (FLC) to maintain the FESS operating within its limits. In [14], the authors presented a voltage and frequency comparison in different scenarios of combinations between diesel, dump load, and FESS and they proposed a solution for the active power surpluses in a wind-diesel power system utilizing FESS and dump load using a proportional-integral controller. To regulate the power entering into the grid, it has been examined in [9] to combine a squirrel cage induction machine-based FESS with a Permanent Magnet Synchronous Generator (PMSG)-based wind generator.

A high-speed FESS has been carefully modeled and continuously simulated in [15]. The grid voltage and frequency can be supported quickly and effectively by the high-speed FESS during unexpected events. For primary frequency control studies, a FESS practical model has been proposed in [16]. The results of the proposed FESS's implementation showed that the FESS was suitable for primary frequency control and voltage regulation.

A detailed model of the FESS structure and the application of two control strategies (V/f and PQ control) were shown in [17]. Additionally, two complimentary controllers conventional PI and fuzzy controllers were suggested for the V/f control method to improve the microgrid frequency and voltage stability. A typical low-voltage network with FESS was simulated for four different scenarios. It has been demonstrated that in an islanded microgrid, fuzzy controllers perform better than traditional PI controllers. In[18], the authors provided a comprehensive model for FESS and used MATLAB Simulink to investigate various scenarios. The simulation findings showed that FESS can produce power even in the event of a utility grid interruption and can tolerate fluctuations in load, PVs, and wind.

The contributions made by this paper are summarized as follows: (1) Managing the frequency and voltage on a 14-bus isolated microgrid using FESS under various load curves and different wind speeds. (2) Designing the modeling and control architecture for fuzzy-controlled FESS. (3) FESS allows isolated microgrids to reduce their reliance on diesel generators when demand or wind conditions vary. The remaining portions of the paper are structured as follows: The problem description and solution process are covered in Section 2. The modeling of the microgrid components under study and the control strategy of the proposed FESS are described in Section 3. In Section 4, the simulation findings are examined and commented on. The study's general conclusion and future work are presented in Section 5 and Section 6, respectively.

II. Problem Description and Solution Process

Microgrids have demonstrated their effectiveness in a wide range of applications with different RESs. However, microgrid control in islanded mode is so difficult compared with a grid-connected mode due to the systems' susceptibility to voltage as well as frequency deviations, less equivalent inertia, higher complexity, and weaker grid compared to conventional utility power grid, in addition to the intermittent nature of the RESs. A robust control mechanism is consequently required to stabilize the grid's frequency and voltage. Because of this, WECSs require ESSs to solve these issues, particularly those involving voltage and frequency stability [19]. In this study,

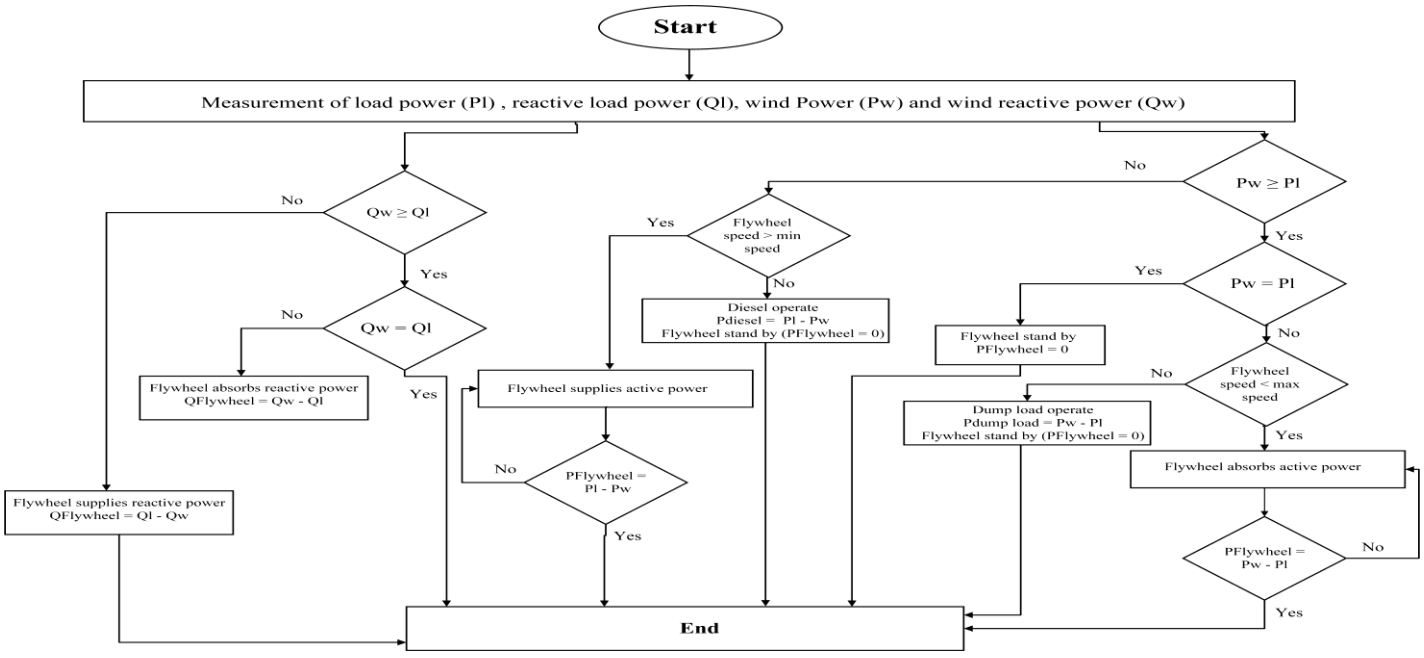

Fig. 1 Flowchart for the solution process

FESS is utilized to mitigate voltage and frequency fluctuations resulting from load or generation variations.

Fig. 1 displays the solution process. the initial stage of recording wind and load power measurements. The wind's active power is compared to the active power of the load. FESS will operate in standby mode if they are equal. In the event that the flywheel speed is higher than its minimal value and the load power is larger than the wind power, FESS will come in to make up the difference. In the absence of this, diesel will step in to make up the difference in power. In contrast, if wind power exceeds load power, FESS will intervene to absorb the extra power as long as its speed is below the maximum value; otherwise, a dump load will do the same. The reactive power of the load and the wind are again compared. If they are equivalent, FESS will operate in a unity power factor mode. FESS will make up for any discrepancy if the value of either of them differs from the other.

III. CONFIGURATION OF THE STUDIED MICROGRID SYSTEM

The studied system, shown in Fig. 2, is a 14-bus distribution system consisting of the wind energy system as the main power source with FESS and a Diesel Generator (DG) unit with a dump load for emergency events. MATLAB Simulink package is used to simulate the studied system and Table 1 shows the studied system parameters.

A. Modeling of Wind Power Generation System

Wind energy is defined as the kinetic energy of a moving air mass, where a wind turbine converts this kinetic energy into mechanical motion that may be utilized to operate the machine directly or to operate a generator to generate electricity directly [20].

The mechanical power, P_m of the wind turbine can be represented by (1) [21].

$$P_m = \frac{1}{2}\,\rho\pi R^2 v^3 Cp\,(\lambda\,,\beta) \tag{1}$$

where ρ, R, v, Cp, β, and λ are air density, rotor radius, wind speed, power coefficient, pitch angle, and tip speed ratio. The tip speed ratio, λ is given by (2).

$$\lambda = \frac{\Omega\, R}{v} \tag{2}$$

where Ω is the angular speed of the turbine.

The power coefficient, Cp specifies the percentage of wind power that may be transformed into mechanical power by the wind turbine. Cp can be specified as a function of pitch angle, β and the tip speed ratio, λ by (3) and (4) [22][23].

$$C_{P(\lambda,\beta)} = C_1\left(\frac{C_2}{\lambda_i} - C_3\beta - C_4\right)e^{\frac{-C_5}{\lambda_i}} + C_6\lambda \tag{3}$$

$$\frac{1}{\lambda_i} = \frac{1}{\lambda+0.08\beta} - \frac{0.035}{\beta^3+1} \tag{4}$$

where C_1 to $C_6$are constants and given by 0.5176, 116, 0.4, 5, 21, and 0.0068, respectively [24], [25].

A doubly fed induction generator (DFIG) is a variable-speed wind generator that can respond to a broad variety of wind speeds.

TABLE.1 Parameter of the studied power system

System voltage	**25 kV**
System frequency	**60 Hz**
Wind turbine:	
Nominal mechanical input	**6×1.5 MW**
Rated wind speed	**15 m/s**
Air density	**1.22 Kg/m^3**
Number of blades	**3**
Maximum power factor Cp max	**0.42**
optimal tip speed ratio	**7.3**
Wind generator:	
Rated power P_{wind}	**6×1.5/0.9 MW**
Stator resistance R_s	**0.023 pu**
Stator Inductance L_s	**0.18 pu**
Rotor resistance R_r	**0.016 s**
Rotor Inductance L_r	**0.16 pu**
Mutual Inductance M	**2.9 pu**
Pole pair	**3**
Emergency diesel	
Rated power	**10 MVA**
Parameters of each FESS unit (10 Units are used)	
Rated power	**1 MVA**
Rated Energy	**60 MJ**
Inertia Constant	**705 Kg.m^2**
Rated speed $\Omega_{nominal}$	**377 rad/s**
DC-bus capacitance	**80 mF**
Load	
Rated power	**8.98MW/2.55MVAR**
Dump load	
Rated power	**0-4.5 MW**

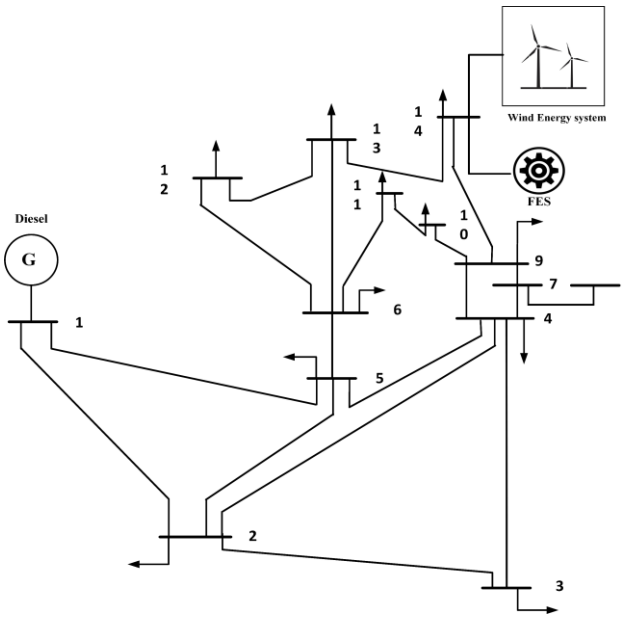

Fig.2 The studied microgrid system

To enhance energy conversion efficiency, DFIG may continually adjust its rotational speed in response to wind speed. The stator of DFIG is directly linked to the grid. However, the rotor of the DFIG is connected to the grid independently via a partial scale converter system that runs at 30 percent of the rated power of the DFIG to reduce the size and cost of the converter system. The converter system is made up of two voltage source converters, a Rotor Side Converter (RSC) and a Grid Side Converter (GSC), which are linked together by a DC link capacitor. This converter system expands the speed range of the DFIG and regulates the generator speed to catch the maximum power extracted from the wind turbines [26]. A typical schematic diagram of the DFIG wind turbine is shown in Fig. 3.

As shown in Fig. 4 [27], the voltages of DFIG can be obtained, in direct (d) and quadrature (q) axis references, by equations (5) – (8)[28]:

$$v_{ds} = R_s i_{ds} + \frac{d}{dt}\emptyset_{ds} - \omega_s \emptyset_{qs} \quad (5)$$

$$v_{qs} = R_s i_{qs} + \frac{d}{dt}\emptyset_{qs} + \omega_s \emptyset_{ds} \quad (6)$$

$$v_{dr} = R_r i_{dr} + \frac{d}{dt}\emptyset_{dr} - (\omega_s - \omega)\emptyset_{qr} \quad (7)$$

$$v_{qr} = R_r i_{qr} + \frac{d}{dt}\emptyset_{qr} + (\omega_s - \omega)\emptyset_{dr} \quad (8)$$

where v, i, R, and $\emptyset$ are the voltage, current, resistance, and flux. And s, r are subscripts for stator and rotor, respectively. d, q are subscripts for the d and q components, respectively.

The active and reactive powers of the stator and rotor can be expressed by (9) – (12) [29].

$$P_s = \frac{3}{2}(v_{ds} i_{ds} + v_{qs} i_{qs}) \quad (9)$$

$$Q_s = \frac{3}{2}(v_{qs} i_{ds} - v_{ds} i_{qs}) \quad (10)$$

$$P_r = \frac{3}{2}(v_{dr} i_{dr} + v_{qr} i_{qr}) \quad (11)$$

$$Q_r = \frac{3}{2}(v_{qr} i_{dr} - v_{dr} i_{qr}) \quad (12)$$

where P and Q are the active and reactive powers, respectively.

The total output active and reactive powers are given by (13) and (14) and the electromagnetic torque, T_{em} can be obtained by (15) [28].

$$P = P_s + P_r \quad (13)$$

$$Q = Q_s + Q_r \quad (14)$$

$$T_{em} = p.(\emptyset_{ds} i_{qs} - \emptyset_{qs} i_{ds}) \quad (15)$$

where p is the total number of pole pair

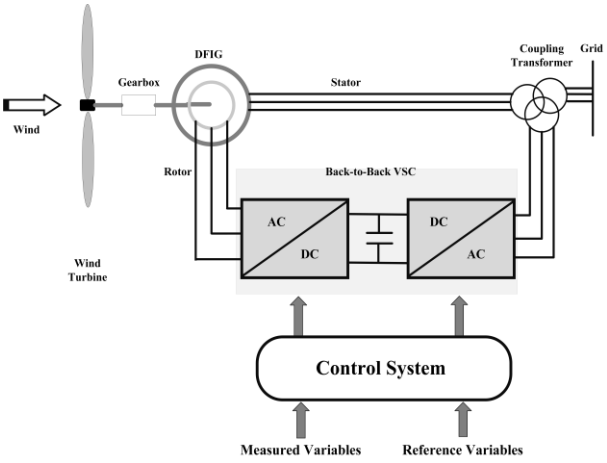

Fig.3 Typical schematic diagram of DFIG

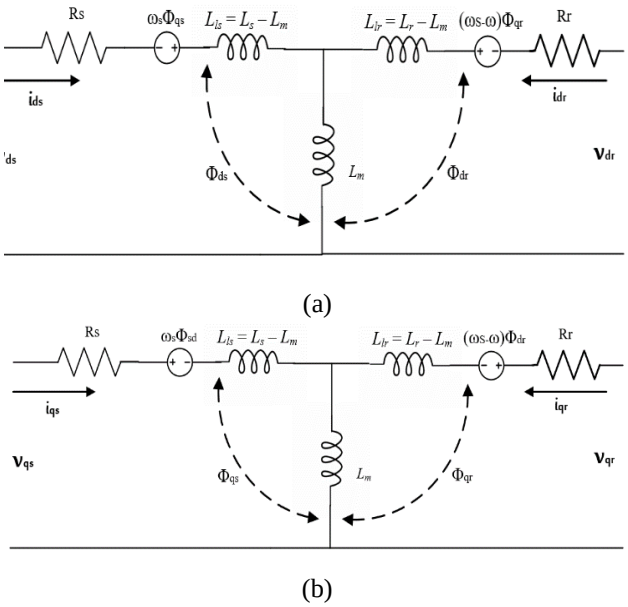

(a)

(b)

Fig. 4 Dynamic d-q equivalent circuit of DFIG: (a) the d-axis equivalent circuit; (b) the q-axis equivalent circuit

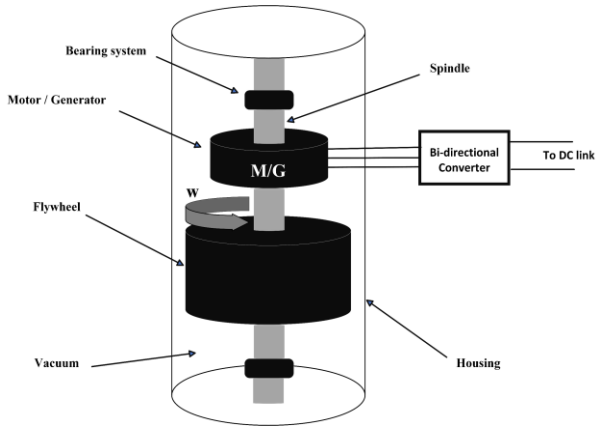

Fig. 5 Schematic diagram of FESS

B. Modeling and Control of FESS

A flywheel is an electromechanical device that stores kinetic energy. It consists of a rotating disk connected to an electrical machine having two operating modes, a motor and a generator mode of operation. When the machine works as a motor, energy flows from the network to the flywheel which increases flywheel speed and stores mechanical energy. It works as a generator by flowing the energy from the flywheel to the network causing a decrease in the flywheel speed and its stored energy [30]–[32].

1) Flywheel Model Configuration

A schematic diagram of FESS is shown in Fig. 5. Flywheel stored energy, E can be expressed by (16) [11].

$$E = \frac{1}{2} J \, {\Omega_f}^2 \tag{16}$$

where J and Ω_f are the inertia and speed of the flywheel, respectively.

Only a portion of the flywheel's energy can be utilized, and this energy E_u can be calculated from the permitted speed variations by (17) [11].

$$E_u = \frac{1}{2} J \, (\Omega_{max} - \Omega_{min})^2 \tag{17}$$

where Ω_max and Ω_min are the flywheel maximum and minimum speeds, respectively. In this study, Ω_max and Ω_min, have values of 1.3 and 0.7 of rated flywheel speed Ω_f respectively [33].

As previously stated, the primary component of the flywheel is the electrical machine. The induction machine, permanent magnet machine, and variable reluctant machine are all familiar electrical machines used in FESS [31][34]. Among these types, the doubly fed induction machine (DFIM) has currently been utilized in FESS due to its flexible control and reduced power converter rating [34]. DFIM modeling was previously expressed in (5) – (8).

2) Flywheel Control System

The DFIM vector control is activated to manage the energy exchanged between the FESS and the grid [23].

a) Rotor Side Converter Control

The RSC controller individually manages the active and reactive powers of DFIM by independently manipulating the rotor currents [35].

By choosing a d-q reference frame related to the stator field and synchronizing it with the stator flux, $\emptyset_{sf}$, DFIM stator voltages and flux can be simplified by (18) – (21), when the stator resistance is neglected.

$$v_{fds} = 0 \tag{18}$$

$$v_{fqs} = \omega_s \emptyset_{fds} = v_{fs} \tag{19}$$

$$\emptyset_{fds} = \emptyset_{fs} = L_s i_{fds} + M i_{fdr} \tag{20}$$

$$\emptyset_{fqs} = 0 = L_s i_{fqs} + M i_{fqr} \tag{21}$$

where v_f, i_f, $\emptyset_f$, L and M are the voltage, current, flux, self-inductance, and mutual inductance, respectively.

The stator powers, P_{fs} and Q_{fs}, electromagnetic torque, T_{fem} and rotor voltages, V_{fdr} and V_{fqr} are expressed by (22) – (27) [36].

$$P_{fs} = -\frac{3}{2} V_{fs} \frac{M_f}{L_{fs}} . i_{fqr} \tag{22}$$

$$Q_{fs} = \frac{3}{2} (V_{fs} \frac{\emptyset_{fs}}{L_{fs}} - V_{fs} \frac{M_f}{L_{fs}} . i_{fdr}) \tag{23}$$

$$T_{fm} = -\frac{3}{2} P_f \frac{M_f}{L_{fs}} \emptyset_{fs} . i_{fqr} \tag{24}$$

$$v_{fdr} = R_{fr} i_{fdr} + \sigma L_{fr} \frac{d}{dt} i_{fdr} - s_f \omega_{fs} \sigma L_{fr} i_{fqr} \tag{25}$$

$$v_{fqr} = R_{fr} i_{fqr} + \sigma L_{fr} \frac{d}{dt} i_{fqr} + s_f \omega_{fs} \sigma L_{fr} i_{fdr} + s_f \frac{M_f . \emptyset_{fs}}{L_{fs}} \tag{26}$$

$$\sigma = 1 - \frac{{M_f}^2}{L_{sf} . L_{rf}} \tag{27}$$

where ω_{fs}, σ, P_f and s are the synchronous electrical speed, leakage coefficient, number of pole pairs, and generator slip, respectively.

From (22) and (23), the reference rotor currents i_{fdr_ref} and i_{fqr_ref} are obtained as a function of the active power reference P_{fs_ref} and reactive power reference Q_{fs_ref} [35]. The complete rotor side controller is shown in Fig. 6.

b) Grid Side Converter Control

The GSC controller is used to keep constant power on the grid by adjusting the DC link voltage and can also be used to control the system power factor [35].

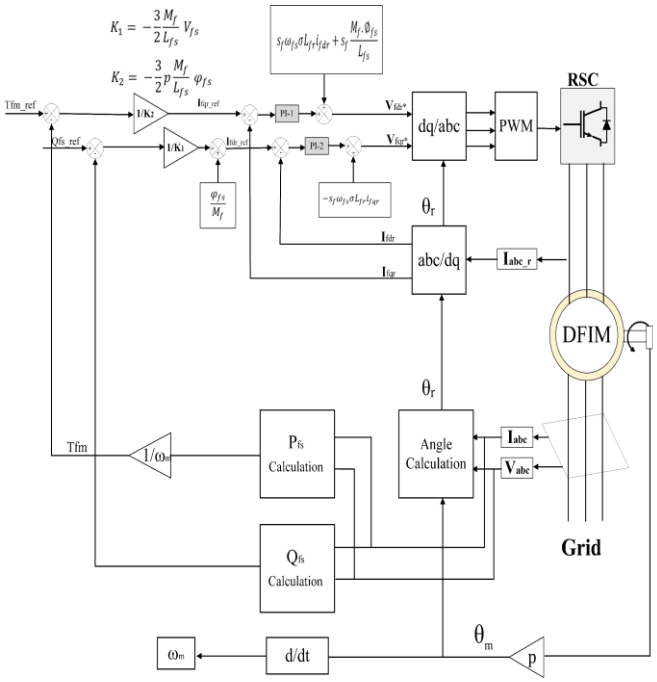

Fig. 6 Rotor side converter controller

A complete grid converter and its controller are shown in Fig. 7 [3]. The GSC is connected to the grid through an RL filter to reduce the current harmonics. The d-q voltage equations can be expressed by (28) and (29)[13].

$$v_{fsd} = R_f i_{fd} + L_f \frac{di_{fd}}{dt} - \omega_s L_f i_{fq} + v_{fd} \quad (28)$$

$$v_{sq} = R_f i_{fq} + L_f \frac{di_{fq}}{dt} + \omega_s L_f i_{fd} + v_{fq} \quad (29)$$

where i_f, R_f, L_f are the stator current, filter resistance, and filter inductance, respectively.

By modifying the grid, voltage is to be oriented along the d-axis direction, so the q-axis component equals zero. Equations (9) and (10), can be set as follows [21]:

$$P_{fs} = \frac{3}{2}(v_{fds} i_{fds}) \quad (30)$$

$$Q_{fs} = -\frac{3}{2}(v_{fds} i_{fqs}) \quad (31)$$

Based on the power balance theory on both sides of the GSC, the DC link voltage control loop is created, and the q-axis component equals zero. This is expressed in (32) and (33).

$$V_{dc} I_{dc} = V_{fds} I_{fds} + V_{fqs} I_{fqs} \quad (32)$$

$$V_{dc} I_{dc} = V_{fds} I_{fds} \quad (33)$$

Based on (33), V_{dc} can be controlled by I_{ds}. The difference between DC-link voltage and DC-link voltage reference is applied to the PI controller to get the reference value of I_{ds}. However, I_{qs} may be used to control the reactive power transfer to/from the source side converter. Reactive power through the source side converter is typically set to zero for unity power factor operation [37].

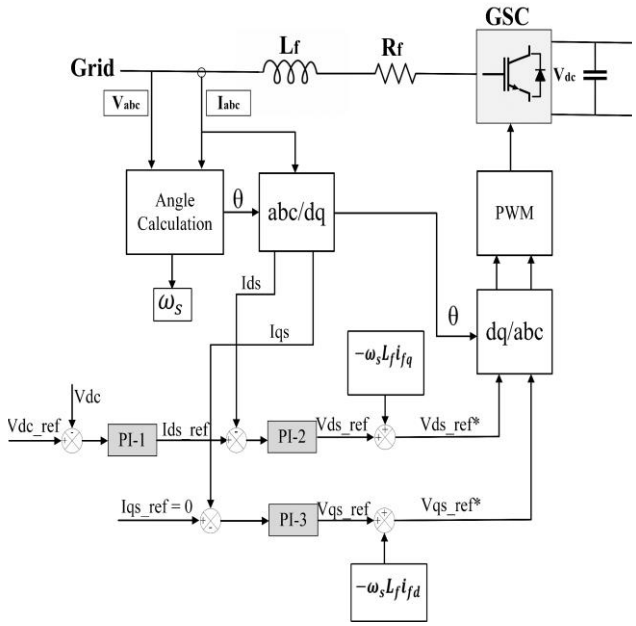

Fig. 7 Grid side converter controller

c) Fuzzy Logic Controller (FLC) to Control FESS Power

FLC is a formal framework for representing, manipulating, and executing human knowledge about system control without the necessity for a full system mathematical model [38]. A fuzzy controller's basic idea is to enable input-output interactions based on fuzzy rules.

The first step in designing FLC is to determine the inputs and outputs of the controller. Essentially, it is needed to ensure that the controller has access to the necessary data to make appropriate decisions as well as achieve high-performance operations. Once the controller inputs and outputs have been determined, the reference inputs must be determined. After all fuzzy inputs and outputs are well-defined, the fuzzification process uses a lookup in one or more membership functions to transform each input set of data into a degree of membership that creates fuzzy inputs by combining a crisp input with a stored membership function [39]. There are several commonly used membership functions (triangular, normal distribution, and trapezoidal membership functions) [40]. In this study, FLC is built by a Gaussian membership function (MF). Equation (34) expresses the Gaussian MF curve.

$$\mu_A(x) = e^{-(\frac{x-a}{b})^2}, \qquad b > a \quad (34)$$

where a, b are parameters representing the center of the curve peak and the width of the curve, respectively.

After that, a set of IF-THEN rules make up a fuzzy rule base, which serves as the brain of the fuzzy system. The process, known as the fuzzy inference mechanism, uses the rule base to determine the fuzzy output. The final step in FLC is called the defuzzification process. The control rule is related to a physical plant, which needs to be controlled by a defuzzification module. The defuzzification module functions as a transformer to change the fuzzy controller output to values that the plant can accept. So, the defuzzification process is the reverse of the fuzzification process [41].

FLC is used in this study to control the power transfer between FESS and the microgrid system. FLC of FESS has two inputs and one output. The first input (dP) can be calculated as the difference between wind power and load power. and that input has a minimum and maximum value of (-10, 10 MW) which is system capacity. The load power can be estimated by measuring the change in diesel output power in case of a change in the value of wind output power due to the climate conditions The second input is $d\Omega$, which shows the amount of change of FESS current speed from the rated speed. $d\Omega$ can be expressed by (35):

$$d\Omega = 1 - \frac{\Omega_f}{\Omega_{nominal}} \quad (35)$$

where Ω_f and $\Omega_{nominal}$ are flywheel current speed and flywheel rated speed, respectively. In this study, $d\Omega$ have a minimum and maximum value of (-0.3, 0.3) which is the minimum and maximum allowable flywheel speed ± 0.3 of rated speed.

The output of FLC is the reference power entering the voltage source converter (VSC) of the flywheel and it takes a value between (-10 and 10 MW).

Both input and output variables are represented by a set of seven Gaussian MFs, as shown in Fig. 8. According to the rule base shown in Table 2, FLC manages fuzzy inference.

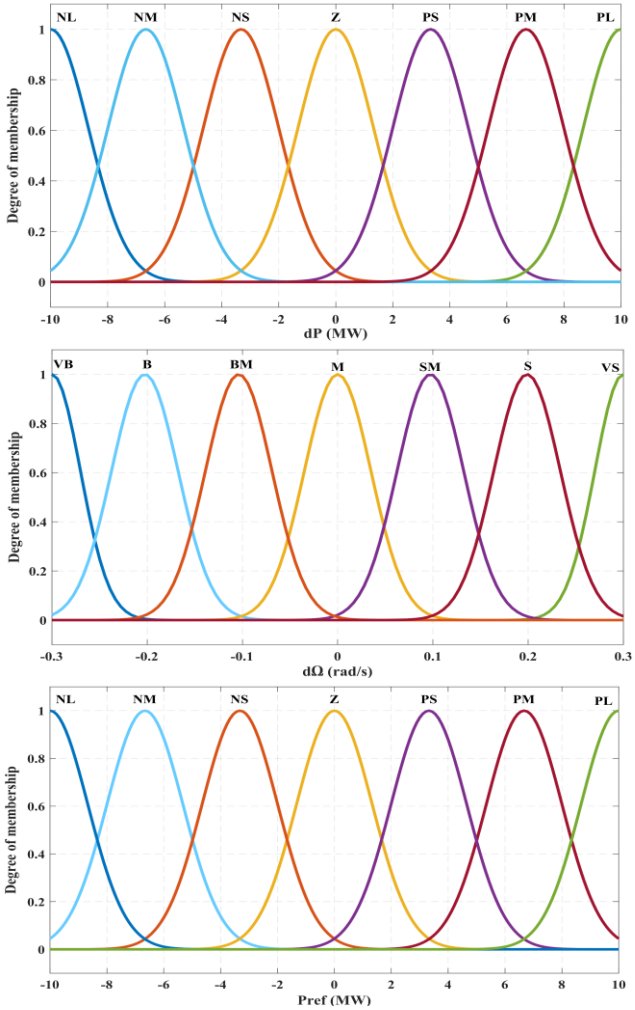

Fig. 8 MFs for inputs and output of FLC Input1 (dP), Input2 ($d\Omega$) and Output (Pref).
NL(Negative Large), NM(Negative Medium), NS(Negative Small), Z(Zero), PL(Positive Large), PM(Positive Medium), PS(Positive Small), VB(Very Big), B(Big), BM(BigMedium), SM (Small Medium), S(Small), VS(Very Small)

TABLE.2 Rule-based look-up table for FLC

dp / $d\Omega$	NL	NM	NS	Z	PS	PM	PL
VB	NL	NM	NS	Z	Z	Z	Z
B	NL	NM	NS	Z	PS	PS	PM
BM	NL	NM	NS	Z	PS	PM	PL
M	NL	NM	NS	Z	PS	PM	PL
SM	NL	NM	NS	Z	PS	PM	PL
S	NM	NS	NS	Z	PS	PM	PL
VS	Z	Z	Z	Z	PS	PM	PL

C. Diesel Modeling

A DG is a reliable backup source to keep regular operations continuing if the needed load power demand cannot be satisfied by the available renewable energy sources and energy storage systems. It is a source that can meet power requirements up to rated power while maintaining a steady frequency.

A DG typically consists of a synchronous generator, an excitation system, and a diesel engine with a governor [42]. Speed governors regulate the diesel engine's speed in order to regulate the system frequency. An actuator plus a speed regulator makes up the speed governor. The actuator operates a fuel valve by transforming the output of the speed regulator into the appropriate signal. As a result, the diesel engine's fuel incoming rate is modified to manage its mechanical power to the necessary value to achieve the desired speed. The synchronous machine supplies reactive power to the whole system in response to the automatic voltage regulator's signals, which is required to maintain the system voltage within acceptable limits [43]. The diesel model is shown in Fig. 9, and it is modeled in MATLAB Simulink using the SimScape toolbox. The Simpowersystem blockset provides this model [44].

D. Dump Load Modeling

When generation from renewable energy sources outpaces consumption, a dump load is employed to dissipate the excess energy. In renewable energy sources like the wind, extra power is generated during periods of high wind velocity. These days, a dump load is used to disperse this power. The surplus energy is wasted in renewable energy plants [45], [46]. In this study, a bank of resistors and a group of semiconductor power switches make up the dump load. The dump load's active power consumption can be managed by closing or opening those power switches, acting as a controlled source of active power. Eight three-phase resistors are used as the dump load in this study, and each one is linked in series with semiconductor switches (one switch in each phase). The appropriate three-phase resistor is attached to/disconnected from the microgrid by closing/opening a set of three switches [47]. The dump load model is shown in Fig. 10, and it is modeled in MATLAB Simulink using the SimScape toolbox. The SymPowerSystem blockset provides this model [44].

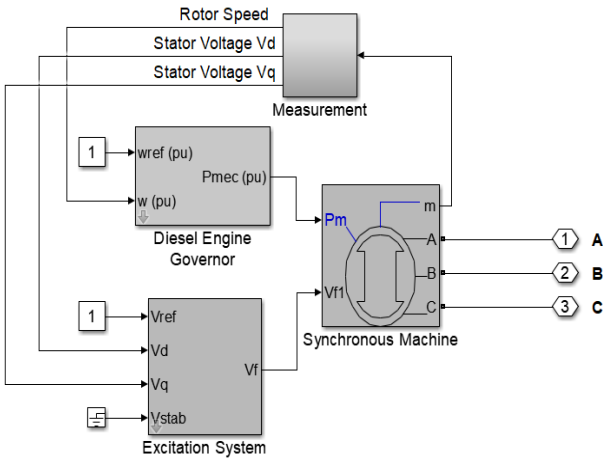

Fig. 9 Emergency Diesel Model

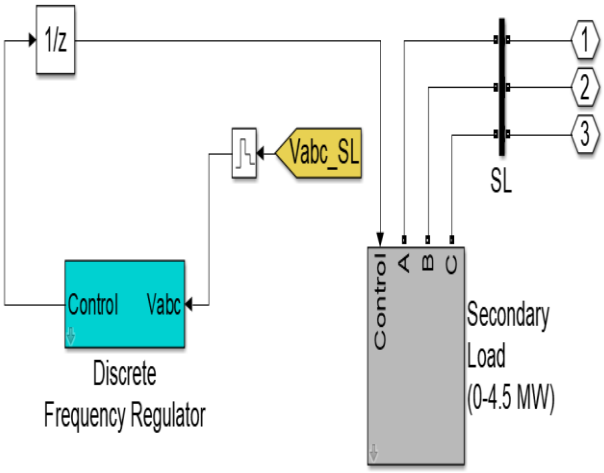

Fig. 10 Dump Load Model

IV. Results and Discussion

In this study, FESS is controlled to mitigate frequency and voltage oscillation in the microgrid system. The total system loads approximately equal 10 MVA and it's fed from a wind turbine (100% penetration). FESS is utilized to balance the generated and absorbed power with a backup 10 MVA emergency DG with a dump load. FESS is applied to overcome the abovementioned problem.

The variations of wind speed and load conditions are studied in two scenarios: wind variations only and load variations only. The results for both scenarios show an improvement in voltage and frequency. For each scenario, there are three configurations, and every voltage and frequency finding of the three configurations is compared to each other. The first configuration, referred to as "only diesel" consists of a standalone microgrid system that is entirely powered by wind energy and has a DG as a backup source. The second arrangement, known as "diesel dump load," is similar to the first configuration but includes a dump load. The final arrangement, named "FESS" consists of an isolated microgrid system connected to FESS whose operation is totally powered by wind energy.

A. Variable Loads – Constant Generation

The studied system, shown in Fig. 2, is tested in this scenario with variable loads and constant wind speed. The output active and reactive power of the wind turbine and system load, in this scenario, are shown in Fig. 11. The voltage and frequency of the microgrid system for the three examined configurations (only diesel/ diesel dump load/ FESS) are discussed in Fig. 12 and Fig. 13.

Fig. 12 shows voltage variation in all three configurations. The maximum and minimum allowable voltages in a typical system should not deviate from the nominal voltage of the system by more than 5% and -10%, respectively[42]. When FESS is applied, voltage fluctuations are smaller compared with the other two configurations although the voltage deviation is acceptable for the three cases.

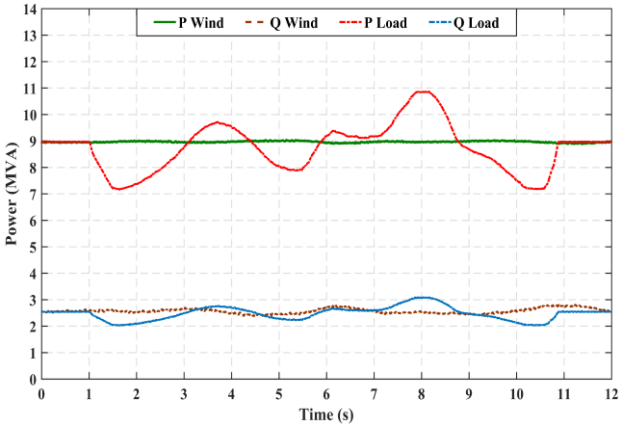

Fig. 11 Wind and load powers for Scenario 1

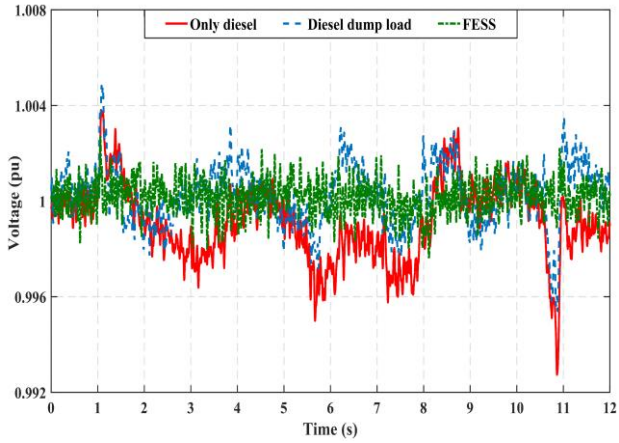

Fig. 12 System voltage for Scenario 1

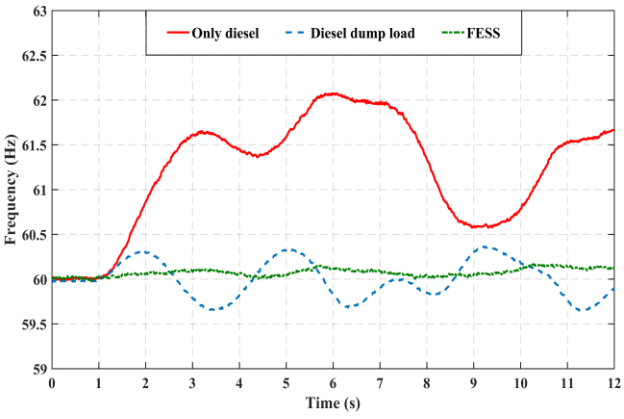

Fig. 13 System frequency for Scenario 1

Moreover, Fig. 13 shows that the frequency variation in the case of FESS is considered the least one. The percentages of minimum and maximum overshoot values of frequency in the case of diesel dump load are 0.58% and 0.62%, respectively. However, in the case of FESS, these values are 0.15% and 0.18%, respectively. This indicates the superiority of applying FESS.

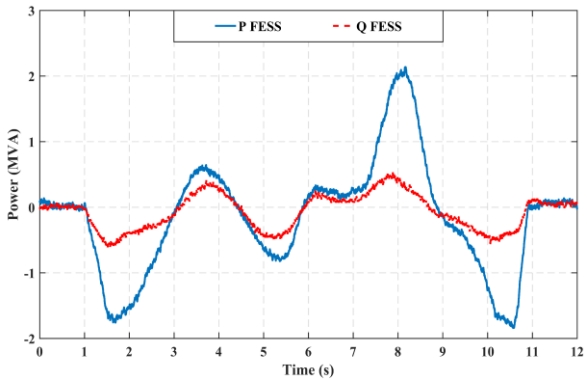

Fig. 14 Active/reactive power of FESS for Scenario 1

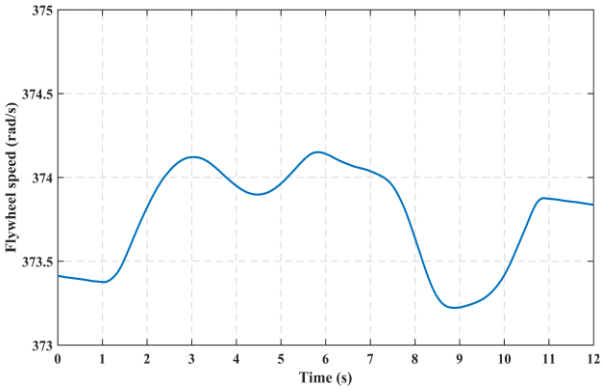

Fig. 15 Flywheel speed for Scenario 1

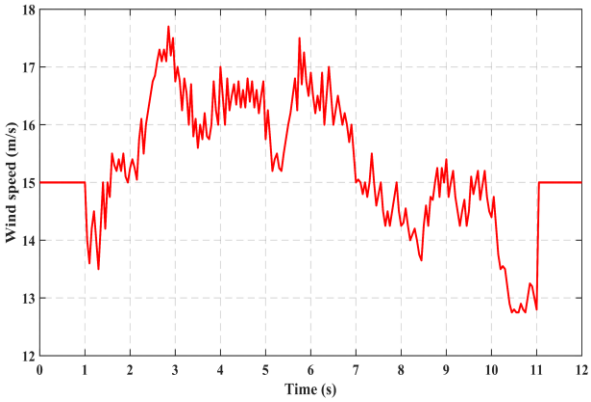

Fig. 16 wind speed variation for Scenario 2

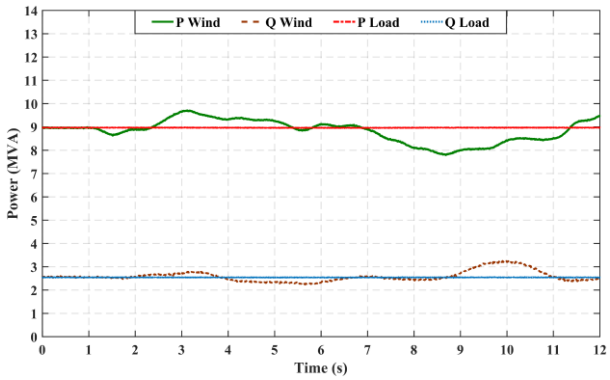

Fig. 17 Wind and load powers for Scenario 2

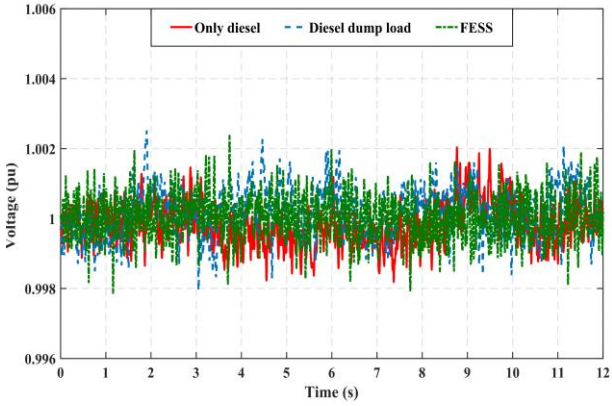

Fig. 18 System voltage for Scenario 2

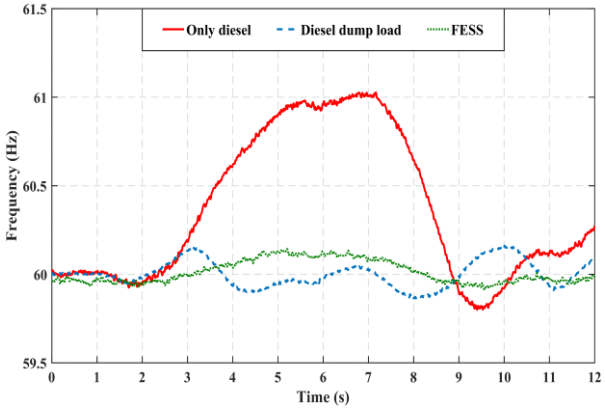

Fig. 19 System frequency for Scenario 2

Fig. 14 shows the active and reactive powers of FESS for scenario 1. It is clear that the FESS active and reactive powers compensate for the power difference between generation and demand powers, which indicates that FESS was able to handle load power fluctuations in this scenario. Flywheel speed is shown in Fig. 15. Also, it is within the permitted range (±30% of the rated flywheel speed value).

B. Constant Loads – Variable Generation

In this scenario, the studied system is tested with constant load values and short variations in wind speed, as presented in Fig. 16. The output active and reactive powers of the wind turbine and system load in this scenario are shown in Fig. 17.

The response of voltage and frequency for the three examined cases are discussed in Fig. 18 and Fig. 19, respectively. Fig. 18 shows that the voltage deviations for the cases are within the acceptable standard limitations, although the deviation is the smallest one when FESS is applied. Fig. 19 shows that the frequency deviation, when FESS is applied is the smallest one. When a diesel dump load is applied, the minimum and maximum values of frequency are 59.86 Hz and 60.17 Hz, respectively. However, the minimum and maximum values of frequency are 59.91 Hz and 60.13 Hz, respectively, when FESS is applied. This shows that the proposed method can significantly reduce the minimum and maximum overshoots by 34.8% and 21.4%, respectively.

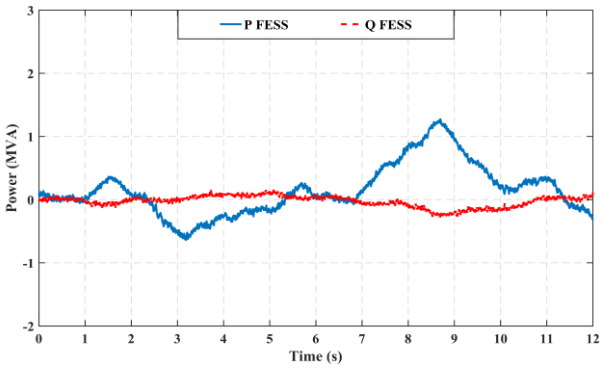

Fig. 20 Active and reactive power of FESS for Scenario 2

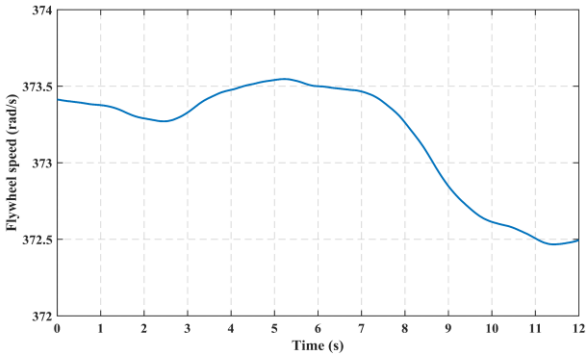

Fig. 21 Flywheel speed for Scenario 2

Fig.20 presents the output active and reactive powers of FESS, which shows that FESS can provide the microgrid with the necessary power to handle wind power fluctuations. Fig. 21 shows the flywheel speed, which is within the permitted range of operation (±30 % of the rated speed value).

V. CONCLUSION

In this study, a proposed control strategy is presented to reduce the voltage and frequency fluctuations caused by loads and wind speed variations in isolated microgrid systems. IEEE 14-bus system is reconstructed for being a microgrid for the present study, which included wind power generation and a backup synchronous diesel generator with dump load. The impact of wind speed and load variations are examined under two different scenarios, namely, the variation in wind speed with constant load and load variation with constant wind speed. FLC is designed to control the charge and discharge of both active and reactive powers of the FESS. Three cases were examined in this study (i.e., diesel generator alone, diesel generator with dump load, and fuzzy-controlled FESS in the presence of the diesel generator-dump load as a backup). To compensate for voltage and frequency variations, the voltage deviations for the first scenario's fluctuating load and constant generation are all within the permitted standard limits, even though the usage of FESS results in the smallest deviation. Furthermore, when it comes to frequency, FESS appears to have the least frequency variation. In the case of diesel dump load, the percentages of lowest and maximum overshoot values of frequency are, respectively, 0.58% and 0.62%. These values are, however, 0.15% and 0.18%, respectively, for FESS. For the second scenario's constant load and variable generation, all three findings of voltage fall within the permitted standard limits. Additionally, when it comes to frequency, FESS is thought to have the least frequency variation. Diesel dump load frequency has percentages for minimum and maximum values of 0.23% and 0.28%, respectively. However, the values are, respectively, 0.15% and 0.21% in the case of FESS. The obtained results demonstrated that the proposed fuzzy-controlled FESS successfully minimized the voltage and frequency fluctuations of the studied microgrid system in both scenarios and maintained their variations within the permitted limitations.

VI. FUTURE WORK

Through additional research, there is still room for the work to be expanded or improved. The suggested FESS makes use of controllers based on FLC and PI control. The effectiveness can be contrasted with that of other advanced controllers, such as neural networks, predictive control, etc. Comparisons between FESS and other well-known storage devices can also be made in various scenarios and with various power systems to ascertain the advantages and disadvantages of each energy storage device.

REFERENCES

[1] H. Abu-Rub, M. Malinowski, and K. Al-Haddad, *POWER ELECTRONICS FOR RENEWABLE ENERGY SYSTEMS, TRANSPORTATION AND INDUSTRIAL APPLICATIONS*, 1st ed., vol. 148. IEEE Press, John Wiley and Sons Ltd, 2014.

[2] M. Mahmoud, M. Ramadan, A. G. Olabi, K. Pullen, and S. Naher, "A review of mechanical energy storage systems combined with wind and solar applications," *Energy Convers Manag*, vol. 210, no. February, p. 112670, 2020, doi: 10.1016/j.enconman.2020.112670.

[3] N. S. Chouhan, "Doubly fed induction generator with integrated energy storage system for smoothening of output power," MISSOURI UNIVERSITY OF SCIENCE AND TECHNOLOGY, 2010.

[4] M. Metwally Mahmoud, "Improved current control loops in wind side converter with the support of wild horse optimizer for enhancing the dynamic performance of PMSG-based wind generation system," *International Journal of Modelling and Simulation*, 2022, doi: 10.1080/02286203.2022.2139128.

[5] F. Díaz-González, A. Sumper, O. Gomis-Bellmunt, and R. Villafáfila-Robles, "A review of energy storage technologies for wind power applications," *Renewable and Sustainable Energy Reviews*, vol. 16, no. 4, pp. 2154–2171, 2012, doi: 10.1016/j.rser.2012.01.029.

[6] S. P. Bihari *et al.*, "A Comprehensive Review of Microgrid Control Mechanism and Impact Assessment for Hybrid Renewable Energy Integration," *IEEE Access*, vol. 9, pp. 88942–88958, 2021, doi: 10.1109/ACCESS.2021.3090266.

[7] M. G. Cendoya, G. M. Toccaceli, P. E. Battaiotto, and R. J. Vignoni, "Microgrid for remote areas with Water Pumping, based on wind-diesel der and Energy Storage," *2015 IEEE PES Innovative Smart Grid Technologies Latin America, ISGT LATAM 2015*, pp. 154–159, 2016, doi: 10.1109/ISGT-LA.2015.7381145.

[8] C. Jin, X. Jiang, G. Zhong, and X. Li, "Research on coordinated control strategy of flywheel energy storage array for island microgrid," *2017 IEEE Conference on Energy Internet and Energy System Integration, EI2 2017 - Proceedings*, vol. 2018-Janua, pp. 1–6, 2017, doi: 10.1109/EI2.2017.8245616.

[9] M. Mansour, M. N. Mansouri, S. Bendoukha, and M. F. Mimouni, "A grid-connected variable-speed wind generator driving a fuzzy-controlled PMSG and associated to a flywheel energy storage system," *Electric Power Systems Research*, vol. 180, no. November 2019, p. 106137, 2020, doi: 10.1016/j.epsr.2019.106137.

[10] J. Li, J. Bi, G. Yan, Y. Ge, and P. Jin, "Research on improving power quality of wind power system based on the flywheel energy storage system" vol. 1, pp. 10–13, 2016.

[11] C. Carrillo, A. Feijóo, and J. Cidrás, "Comparative study of flywheel systems in an isolated wind plant," *Renew Energy*, vol. 34, no. 3, pp. 890–898, 2009, doi: 10.1016/j.renene.2008.06.003.

[12] J. G. Ndirangu, J. N. Nderu, A. M. Muhia, and C. M. Maina, "Power quality challenges and mitigation measures in grid integration of wind energy conversion systems," *2018 IEEE International Energy Conference, ENERGYCON 2018*, pp. 1–6, 2018, doi: 10.1109/ENERGYCON.2018.8398823.

[13] M. Nadour, A. Essadki, and T. Nasser, "Power Smoothing Control of DFIG Based Wind Turbine using Flywheel Energy Storage System," *2020 International Conference on Electrical and Information Technologies, ICEIT 2020*, pp. 0–6, 2020, doi: 10.1109/ICEIT48248.2020.9113213.

[14] R. Sebastián and R. Peña-Alzola, "Flywheel energy storage and dump load to control the active power excess in a wind diesel power system," *Energies (Basel)*, vol. 13, no. 8, 2020, doi: 10.3390/en13082029.

[15] S. Karrari, M. Noe, and J. Geisbuesch, "High-speed Flywheel Energy Storage System (FESS) for Voltage and Frequency Support in Low Voltage Distribution Networks," *2018 IEEE 3rd International Conference on Intelligent Energy and Power Systems, IEPS 2018 - Proceedings*, vol. 2018-Janua, pp. 176–182, 2018, doi: 10.1109/IEPS.2018.8559521.

[16] D. Peralta, C. Canizares, and K. Bhattacharya, "Practical Modeling of Flywheel Energy Storage for Primary Frequency Control in Power Grids," *IEEE Power and Energy Society General Meeting*, vol. 2018-Augus, no. November 2017, pp. 1–5, 2018, doi: 10.1109/PESGM.2018.8585844.

[17] A. A. K. Arani, B. Zaker, and G. B. Gharehpetian, "A control strategy for flywheel energy storage system for frequency stability improvement in islanded microgrid," *Iranian Journal of Electrical and Electronic Engineering*, vol. 13, no. 1, pp. 10–21, 2017, doi: 10.22068/IJEEE.13.1.2.

[18] A. Saleh, A. Awad, and W. Ghanem, "Modeling, Control, and Simulation of a New Topology of Flywheel Energy Storage Systems in Microgrids," *IEEE Access*, vol. 7, pp. 160363–160376, 2019, doi: 10.1109/ACCESS.2019.2951029.

[19] I. Hussain Panhwar *et al.*, "Mitigating power fluctuations for energy storage in wind energy conversion system using supercapacitors," *IEEE Access*, vol. 8, pp. 189747–189760, 2020, doi: 10.1109/ACCESS.2020.3031446.

[20] M. H. Ali, *Wind energy systems: Solutions for power quality and stabilization*. 2017. doi: 10.1201/b11525.

[21] I. Yaichi, A. Semmah, and P. Wira, "Direct power control of a wind turbine based on doubly fed induction generator," *European Journal of Electrical Engineering*, vol. 21, no. 5, pp. 457–464, 2019, doi: 10.18280/ejee.210508.

[22] T. Burton, D. Sharpe, N. Jenkins, and E. Bossanyi, *WIND ENERGY HANDBOOK*, First. Chichester, England: Wiley, 2001.

[23] A. Boumassata, D. Kerdoun, and M. Madaci, "Grid power control based on a wind energy conversion system and a flywheel energy storage system," *Proceedings - EUROCON 2015*, vol. 1, no. 1, pp. 1–6, 2015, doi: 10.1109/EUROCON.2015.7313699.

[24] S. Mensou, A. Essadki, I. Minka, T. Nasser, B. Bououlid Idrissi, and L. ben Tarla, "Performance of a vector control for DFIG driven by wind turbine: real time simulation using DS1104 controller board," *International Journal of Power Electronics and Drive Systems (IJPEDS)*, vol. 10, no. 2, p. 1003, 2019, doi: 10.11591/ijpeds.v10.i2.pp1003-1013.

[25] M. M. Mahmoud, M. Khalid Ratib, M. M. Aly, and A. M. M. Abdel-Rahim, "Wind-driven permanent magnet synchronous generators connected to a power grid: Existing perspective and future aspects," *Wind Engineering*, vol. 46, no. 1, pp. 189–199, Feb. 2022, doi: 10.1177/0309524X211022728.

[26] P. Mukherjee and V. V. Rao, "Effective location of SMES for power fluctuation mitigation of grid connected doubly fed induction generator," *J Energy Storage*, vol. 29, no. March, p. 101369, 2020, doi: 10.1016/j.est.2020.101369.

[27] P. He, F. Wen, G. Ledwich, Y. Xue, and J. Huang, "Investigation of the Effects of Various Types of Wind Turbine Generators on Power-System Stability," *Journal of Energy Engineering*, vol. 141, no. 3, 2015, doi: 10.1061/(asce)ey.1943-7897.0000176.

[28] K. Ghedamsi, D. Aouzellag, and E. M. Berkouk, "Control of wind generator associated to a flywheel energy storage system," *Renew Energy*, vol. 33, no. 9, pp. 2145–2156, 2008, doi: 10.1016/j.renene.2007.12.009.

[29] B. B. M. El Amine, A. Ahmed, M. B. Houari, and D. Mouloud, "Modeling, simulation and control of a doubly-fed induction generator for wind energy conversion systems," *International Journal of Power Electronics and Drive Systems*, vol. 11, no. 3, pp. 1197–1210, 2020, doi: 10.11591/ijpeds.v11.i3.pp1197-1210.

[30] A. A. Khodadoost Arani, G. B. Gharehpetian, and M. Abedi, "Review on Energy Storage Systems Control Methods in Microgrids," *International Journal of Electrical Power and Energy Systems*, vol. 107, no. November 2018, pp. 745–757, 2019, doi: 10.1016/j.ijepes.2018.12.040.

[31] A. G. Olabi, T. Wilberforce, M. A. Abdelkareem, and M. Ramadan, "Critical review of flywheel energy storage system," *Energies (Basel)*, vol. 14, no. 8, pp. 1–33, 2021, doi: 10.3390/en14082159.

[32] R. Sebastián and R. Peña Alzola, "Flywheel energy storage systems: Review and simulation for an isolated wind power system," *Renewable and Sustainable Energy Reviews*, vol. 16, no. 9, pp. 6803–6813, 2012, doi: 10.1016/j.rser.2012.08.008.

[33] A. Abdel-Khalik, A. Elserougi, A. Massoud, and S. Ahmed, "A power control strategy for flywheel doubly-fed induction machine storage system using artificial neural network," *Electric Power Systems Research*, vol. 96, pp. 267–276, 2013, doi: 10.1016/j.epsr.2012.11.012.

[34] M. E. Amiryar and K. R. Pullen, "A review of flywheel energy storage system technologies and their applications," *Applied Sciences*, vol. 7, no. 3, 2017, doi: 10.3390/app7030286.

[35] S. A. Belfedhal, E. M. Berkouk, Y. Meslem, and Y. Soufi, "Modeling and control of wind power conversion system with a flywheel energy storage system and compensation of reactive power," *International Journal of Renewable Energy Research*, vol. 2, no. 3, pp. 528–534, 2012, doi: 10.20508/ijrer.37438.

[36] I. Hamzaoui, F. Bouchafaa, A. Talha, and A. Boukhlifa, "Fuzzy logic control for a speed of a flywheel energy storage system associated the wind generator," *International Aegean Conference on Electrical Machines and Power Electronics, ACEMP 2011 and Electromotion 2011 Joint Conference*, no. September, pp. 537–543, 2011, doi: 10.1109/ACEMP.2011.6490656.

[37] C. M. R. Charles, V. Vinod, and A. Jacob, "Field oriented control of Doubly Fed Induction Generator in wind power system," *2015 IEEE International Conference on Computational Intelligence and Computing Research, ICCIC 2015*, 2016, doi: 10.1109/ICCIC.2015.7435760.

[38] N. Siddique, *Fuzzy control*, vol. 517. 2014. doi: 10.1007/978-3-319-02135-5_5.

[39] J. D. Barrett, *Advanced Fuzzy Logic Technologies in Industrial Applications*, vol. 49, no. 4. 2007. doi: 10.1198/tech.2007.s689.

[40] Y. Zamrodah, *Fuzzy Modeling and Fuzzy Control*, vol. 15, no. 2. 2016.

[41] G. Chen and T. T. Pham, *Introduction to Fuzzy Sets, Fuzzy Logic and Fuzzy Control Systems*, vol. 1999, no. December. 2006.

[42] *IEC 60038*. 2009. [Online]. Available: https://standards.iteh.ai/catalog/standards/sist/bd26a0a9-bf9f-4094-9ab3-